



**HAL**  
open science

## Measuring interdiffusion at an interface between two elastomers with tapping-mode and contact-resonance atomic force microscopy imaging

Bruno Bresson, Maude Portigliatti, Benoit Salvant, Christian Frétigny

### ► To cite this version:

Bruno Bresson, Maude Portigliatti, Benoit Salvant, Christian Frétigny. Measuring interdiffusion at an interface between two elastomers with tapping-mode and contact-resonance atomic force microscopy imaging. *Journal of Applied Polymer Science*, 2008, 109 (1), pp.602-607. 10.1002/app.27914. hal-03130301

**HAL Id: hal-03130301**

**<https://hal.science/hal-03130301>**

Submitted on 3 Feb 2021

**HAL** is a multi-disciplinary open access archive for the deposit and dissemination of scientific research documents, whether they are published or not. The documents may come from teaching and research institutions in France or abroad, or from public or private research centers.

L'archive ouverte pluridisciplinaire **HAL**, est destinée au dépôt et à la diffusion de documents scientifiques de niveau recherche, publiés ou non, émanant des établissements d'enseignement et de recherche français ou étrangers, des laboratoires publics ou privés.

# Measuring Interdiffusion at an Interface Between Two Elastomers with Tapping-Mode and Contact-Resonance Atomic Force Microscopy Imaging

Bruno Bresson,<sup>1</sup> Maude Portigliatti,<sup>2</sup> Benoit Salvant,<sup>2</sup> Christian Fretigny<sup>3</sup>

<sup>1</sup>LPQ/ESPCI CNRS UMR 7142, 10 Rue Vauquelin, 75005 Paris, France

<sup>2</sup>Centre de Technologie Michelin, Ladoux, 23 Place des Carmes Déchaux, 63000 Clermont-Ferrand, France

<sup>3</sup>PPMD/ESPCI CNRS UMR 7615, 10 Rue Vauquelin, 75005 Paris, France

Received 11 May 2007; accepted 11 December 2007

DOI 10.1002/app.27914

Published online 1 April 2008 in Wiley InterScience (www.interscience.wiley.com).

**ABSTRACT:** Despite the common use of tapping-mode atomic force microscopy to image composites or polymer blends, very few studies have focused on the measurement of the interdiffusion at an interface between two polymers in contact. In this study, we show how to assess the interphase between two polymers with two methods. First, stable and robust tapping conditions are established, and the problem of the phase contrast is discussed. Second, a contact-resonance method is presented: the tip in contact with the sam-

ple is electrostatically excited at its resonance frequency by a self-controlled oscillator. The gain and frequency images allow us to measure the interdiffusion width. Both methods (using high and weak mechanical solicitation) give the same assessment of the interdiffusion width. © 2008 Wiley Periodicals, Inc. *J Appl Polym Sci* 109: 602–607, 2008

**Key words:** atomic force microscopy (AFM); elastomers; interfaces; mechanical properties; miscibility

## INTRODUCTION

The reliable measurement of polymer chain interdiffusion at an interface between two polymeric materials in contact is of great importance to many industrial applications. The description of composite materials based on a multilayered or blend elastomer structure, such as tires, requires its precise measurement. The interface between two polymers is a notion demanding precision. For example, two polymer mixtures can simply be put into contact, which leads to chain interdiffusion, or be submitted to a curing process, which leads to interdiffusion and crosslinking phenomena. In this study, butadiene rubber (BR) and styrene-butadiene rubber (SBR) were put into contact, and this BR/SBR couple was subsequently cured. The interphase between the two elastomers is defined by the region in which the value of a given physical property changes from one homogeneous region, with respect to that physical property, to the other. In this study, two atomic force microscopy (AFM) imaging modes were used to assess the interphase width: well-known tapping-mode phase imaging and contact-resonance imaging.

In the tapping mode, the phase shift between the excitation of the cantilever and its response, which is dependent on the energy dissipation of the tip-sample system,<sup>1,2</sup> varies when the tip sweeps a surface with changing mechanical or chemical properties. Surprisingly, despite the common use of phase imaging to show the mechanical contrast in polymer blends,<sup>3–6</sup> almost no study has focused on the assessment of the interphase width.<sup>7</sup> Interphase width measurements are generally carried out on polymer-charge composites<sup>8,9</sup> but not between two polymers. Moreover, the contrast phase inversion issue, pointed out and discussed in the literature,<sup>10–13</sup> can lead to a false assessment of the interphase width. Therefore, particular working conditions must be used. One aim of the article is to properly set some robust acquisition conditions and to discuss the effect of the experimental conditions on the assessment of the interphase width. Therefore, a contact-resonance microscopy method<sup>14–16</sup> has been developed to validate the interphase width measurements; indeed, the agreement of the results obtained by both methods with very high and very weak mechanical solicitation ensures a proper assessment of the interphase width. In the literature, force or displacement modulation methods in the contact mode have been used for analyzing the contact stiffness.<sup>17</sup> Here, a resonant method has been used in which the resonance frequency of the cantilever is shifted because of the contact stiffness.<sup>16,18</sup>

## EXPERIMENTAL

### Materials

The samples were bilayers, made of two elastomer layers 2.5 cm in diameter and 2 mm thick, that were put into contact and subsequently cured. They were supplied by the Michelin Technology Center (Clermont-Ferrand, France) and were studied as received. The polymers used were BR and SBR with respective number-average molecular weights of 120 and 240 kg/mol and respective glass-transition temperatures of  $-105$  and  $-38^\circ\text{C}$ . Two SBR microstructures were chosen to modulate the miscibility of the SBR/BR couple: in the first sample (no. 1), the SBR/BR couple was immiscible, and in the second one (no. 2), the SBR/BR couple was miscible. The samples were prepared by the same procedure to minimize unwanted side effects: they were cut with a razor blade, just before being studied, to get samples with a typical size of  $1 \times 1 \times 10 \text{ mm}^3$  presenting a clear interphase between the two elastomers in the center of the analyzed surface. The identification of the polymer on both sides of the interphase was then direct.

### Tapping-mode imaging

Commercial silicon tapping cantilevers (BS-300, Budget Sensor) (Wetzlar, Germany) were used with a spring constant of about 40 N/m. The resonance frequency of the cantilever typically was 250 kHz. Tapping-mode AFM was performed with a Veeco Dimension 3100 atomic force microscope (Cedex, France). In this study, the excitation frequency, slightly below the resonance frequency of the free cantilever, was such that the ratio  $A(\omega)/A_0(\omega)$  was equal to 0.8, where  $\omega$  stands for the excitation frequency,  $A$  stands for the amplitude of the cantilever, and  $A_0$  stands for the free amplitude of the cantilever. The amplitude, given in nanometers, was obtained from approach-retract calibration of the cantilever in the tapping mode on a silicon wafer. Height and phase images were recorded simultaneously. The phase difference between the cantilever excitation at its resonance and the response of this cantilever was measured by an external lock-in amplifier. The input of the lock-in was the electrical signal arising from the diodes (deflection signal), and the reference signal was the driving excitation signal of the cantilever. It should, however, be noticed that most of the recent commercial instruments offer suitable build-in phase devices.

### Contact-resonance microscopy

The contact-resonance experiments were performed with a home-built device. A silicon nitride V-shaped

cantilever (Veeco NP) with an approximate stiffness of 0.58 N/m was in permanent contact with the sample surface. An electronic feedback loop excited the cantilever at its resonance frequency, whatever the contact conditions were. Excitation was performed via an electrostatic field<sup>16</sup> established between the sample holder and the grounded body of the microscope (Multimode, Veeco). The phase-controlled oscillator that we used was a simplified version of the feedback loops used in dynamic-mode force microscopy.<sup>19</sup> The large frequency shifts involved in the contact-mode resonance method allowed for a simpler design of the loop. The input signal of the home-built device was the electrical signal arising from the diode panel (deflection signal). It was first amplified to a constant amplitude ( $V_0$ ) with an automatic gain control and was then phase-shifted. A constant voltage ( $V_c$ ) was added, and this signal was driven to the sample holder, which was isolated from the ground. The resonance conditions of the loop were fulfilled when the frequency of the signal was identical to that of the cantilever and the phases were matched. The system is illustrated in Figure 1. The tip was embedded in an electric field proportional to the applied voltage,  $V_c + V_0 \cos(\omega t)$ , where  $\omega$  is the frequency and  $t$  is the time. The dielectric tip was submitted to a polarization force proportional to the square of the applied tension  $\{[V_c + V_0 \cos(\omega t)]^2\}$ .<sup>20</sup> This expression gave a term proportional to  $V_c V_0 \cos(\omega t)$ , so that the magnitude of the driving force was controlled by the user. During the scan of the tip, the resonance frequency of the cantilever changed with the mechanical properties of the sample, and so did the quality factor.

The resonance frequency of the cantilever and the gain needed to keep the vibration amplitude of the cantilever constant were independently acquired during the scanning of the surface. The oscillation frequency of the first mode of the cantilever was about 40 kHz. In contact with an elastomer sample, the frequency of this first mode was shifted to a

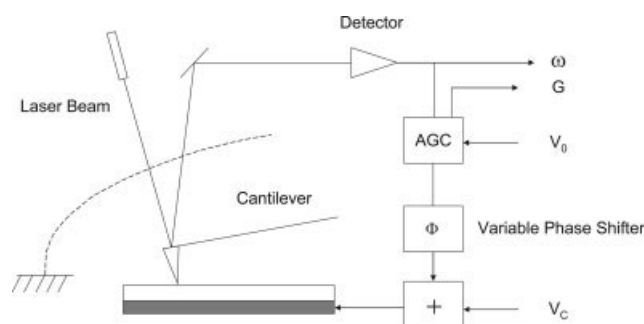


**Figure 1** Schematic diagram of the phase-controlled oscillator setup used for contact-resonance microscopy. G: Gain; AGC: Automatic Gain Controller.

value ranging typically from 100 to 200 kHz, depending on the mechanical properties of the elastomer.

## RESULTS AND DISCUSSION

### Experimental conditions for tapping-mode phase imaging

As shown in the following, the experimental conditions had to be carefully chosen. Indeed, the artifacts in the phase images could prevent us from properly observing the interphase and therefore measuring its width. The experimental conditions of the phase acquisition in the tapping mode are discussed in the following to define robust imaging conditions.

As a first example, a topography image and a phase image of sample 1 are displayed in Figure 2. Only the phase image is split off in two contrasted areas with a sharp transition at the position of  $5.5 \mu\text{m}$ .

Tapping-mode imaging conditions are of primary importance to get reproducible and coherent results. As the principles of the technique rely on the interactions between the tip and the surface, both the excitation frequency and the vibration amplitude determine the phase response of the oscillator. Two oscillation modes are possible: one is linked to an attractive tip-sample interaction, and the other is linked to a repulsive tip-sample interaction.<sup>21</sup> To point out the problems that can occur during the acquisition of a phase image, some phase profiles were acquired with different acquisition parameters. At first, the phase angle profile of the interface was recorded with two different free amplitudes and the

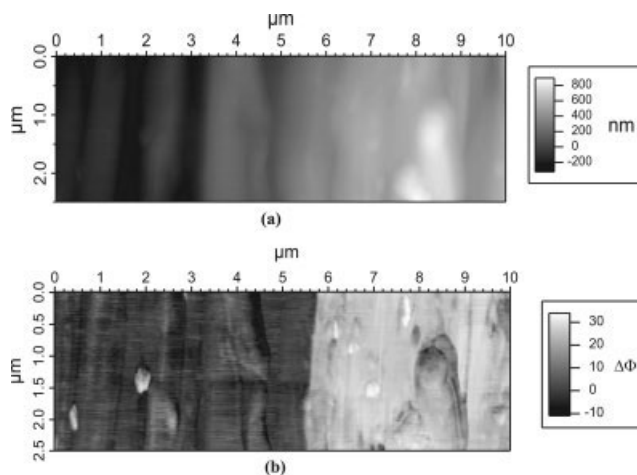


**Figure 2** (a) Topography and (b) phase images of sample 1 acquired with a free amplitude of 175 nm, an  $R_{sp}$  value of 0.85, and a sweeping frequency of 1 Hz. The left part corresponds to BR, and the right part corresponds to SBR. The Z-axis scale is displayed with the corresponding color for the topography image and phase image. The phase angle deviation ( $\Delta\Phi = \Phi - \Phi_0$ ) is displayed in degrees with  $\Phi_0$  equal to the mean phase of the BR part.

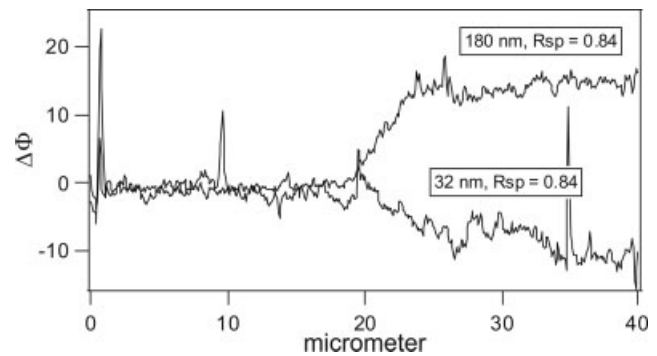


**Figure 3** Two-phase profiles extracted from the two-phase images of the interface of sample 2. The left part corresponds to BR, and the right part corresponds to SBR.  $A_0$  and  $R_{sp}$  are displayed. The phase angle deviation ( $\Delta\Phi = \Phi - \Phi_0$ ) is displayed with  $\Phi_0$  equal to the mean phase of the BR part.

same ratio of  $R_{sp} = A_{sp}/A_0 = 0.84$ , where  $A_{sp}$  stands for the set point value and  $A_0$  stands for the free amplitude value. The phase angle deviation,  $\Delta\Phi = \Phi - \Phi_0$ , is displayed in Figure 3 for sample 2;  $\Phi$  is the current phase angle, and  $\Phi_0$  is the reference phase angle. The result was obtained with a scanning range of  $40 \mu\text{m}$  at a scan frequency equal to 0.5 Hz; the left part corresponds to BR, whereas the right part corresponds to SBR. The chosen phase reference ( $\Phi_0$ ) is equal to the mean phase of the BR (left) part. The contrast inversion suggests that the oscillation mode changed for SBR. For a weak value of the free amplitude (32 nm), the set point vibration amplitude can be reached in the attractive regime: van der Waals forces alone are able to reduce the amplitude of the cantilever to the working value. This regime is to be avoided because a weak mechanical response is expected. High driving amplitudes are then preferred for the interphase studies. In the following, the free amplitude is set to a value close to 180 nm.

To investigate the phase contrast when a phase image is recorded in the tapping mode, the phase

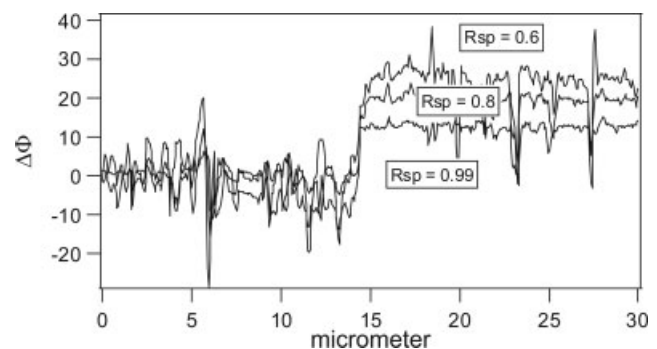


**Figure 4** Phase profile of the interface of sample 1 obtained in the tapping mode with a free amplitude equal to 180 nm, a scan frequency of 0.5 Hz, and different  $R_{sp}$  values. The left part corresponds to BR, and the right part corresponds to SBR. The phase angle deviation ( $\Delta\Phi = \Phi - \Phi_0$ ) is displayed with  $\Phi_0$  equal to the mean phase of the BR part.

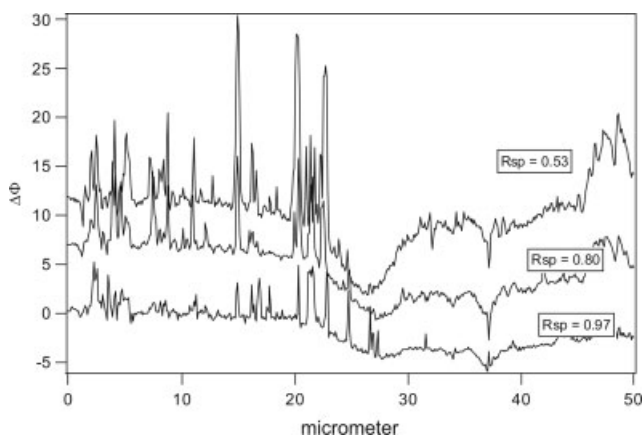


**Figure 5** Sample 2 phase profile extracted from a phase image of the interface with a partially damaged tip. The left part corresponds to BR, and the right part corresponds to SBR.  $A_0$  was equal to 178 nm. The different  $R_{sp}$  values are displayed.

profile of the interphase of sample 1 (narrower than the interphase of sample 2) was studied (see Fig. 4) with various values of the set point ratio and with a high value of the free amplitude (180 nm). The phase contrast increases with the  $R_{sp}$  ratio decreasing. This is in agreement with the relation between the phase measurement and the energy dissipation during a tapping cycle, showing that increasing energy dissipation of the tip-sample interaction leads to an increasing value of the phase.<sup>21</sup> The relative phase between the two elastomers is kept constant whatever the set point values are, showing robust conditions in a regime of repulsive tip-sample interaction. Both a high driving amplitude and a low  $A/A_0$  ratio ensured that we worked in the repulsive tip-sample interaction regime.

As mentioned previously, phase images are a measurement of the dissipation of the interaction between the tip and the surface. The origin of this dissipated energy can be found in adhesion or in the viscoelastic properties of the material. It has been recently shown<sup>22</sup> that, on elastomers, adhesion effects dominate. Then, one expects the tip radius and elastic modulus of the sample to play an important part in the observed contrasts. When the tip is damaged, a larger contact radius may increase the attractive part of the interaction. This may lead to poorer contrasts between both rubbers. Such an effect is exemplified in Figure 5. The profile acquired with a high set point ratio (0.99) is typical of an attractive regime. Increasing  $R_{sp}$  induces a gradual evolution in which the contrast between the two elastomers disappears. In the interphase region, a nonmonotonic behavior can be observed, confirming the complex origin of the phase contrast in these intermediate imaging conditions.

To conclude this section, robust conditions could be found: a high free amplitude (180 nm) and a low

$A/A_0$  ratio ( $<0.8$ ). For an undamaged tip, these conditions guaranteed a good measurement of the interface between the two elastomers for most of the cases by favoring a repulsive interaction regime.

These conditions were used to assess the interphase width for both samples: the interphase width is defined from the profiles by the distance between the two plateaus (Figs. 2 and 3). Both samples were prepared with the same procedure. The only difference lies in the miscibility of the two polymers put into contact: the elastomers in sample 2 were miscible, whereas the elastomers in sample 1 were immiscible. The AFM signal shows an interfacial width of around 8  $\mu\text{m}$  for the miscible couple, whereas the width of the immiscible couple was about 100 nm. In a recent study carried out on elastomer systems,<sup>22</sup> it was shown that in hard tapping conditions, the response of the tip can be affected by an inclusion 80 nm from the tip. This value is inferior to the measured interfacial width between the two elastomers (100 nm). This measurement is then believed to be the true value of the interfacial width. The confirmation of this argument is given in the next section.

It has to be stated that attenuated total reflection/infrared spectroscopy was used on these samples to check that these micrometer-scale gradients measured by AFM indeed were linked to elastomer chain interdiffusion. The miscibility is a fundamental parameter of the interdiffusion of polymers, and a difference in the interfacial width between miscible and immiscible samples was expected. Measuring an interphase width of the order of 10  $\mu\text{m}$  meant that macromolecules in these samples were able to cross distances equal to 1000 times their gyration radius ( $\sim 10$  nm).

### Interphase width measurements by contact-resonance microscopy

This section is devoted to the measurement of the interphase width by contact-resonance microscopy. Displayed in Figure 6 are the topography image, frequency image, and gain image of the BR/SBR interface of sample 2. These images were acquired with a scan size of 30  $\mu\text{m}$  and a sweeping frequency of 0.1 Hz.

The main information extracted from these images is that only the frequency image and the gain image reveal the interphase between the two polymers (BR in the left part and SBR in the right part). Indeed, focusing on the frequency image, for example, we find that the contact-resonance frequency of the cantilever in the BR area is centered at 120 kHz, whereas it is centered at 132 kHz in the SBR area. The profiles extracted from these images in both cases give the same value of the interphase width, which is for sample 2 equal to 8  $\mu\text{m}$  (Fig. 7): the frequency varia-

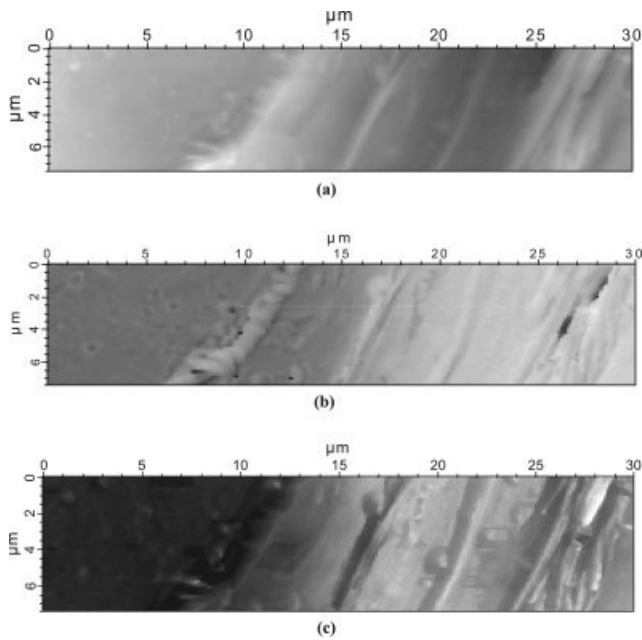


**Figure 6** (a) Topography, (b) frequency, and (c) gain images of sample 2 obtained with electrostatic excitation and with a sweeping frequency of 0.1 Hz.

tion is displayed with a frequency reference (120 kHz) equal to the mean frequency of the cantilever in the BR part (left).

It clearly appears that the resonance frequency on contact is essentially controlled by the mechanical properties of the elastomers. However, it is also observed that the topography, frequency, and gain images are correlated. This correlation between the three images is briefly discussed to properly assess the interphase width.

First, the examination of the profiles of each image indicates that a topography deviation as a sudden increase of the slope if the tip meets with a wall leads to a transient increase of the frequency and a

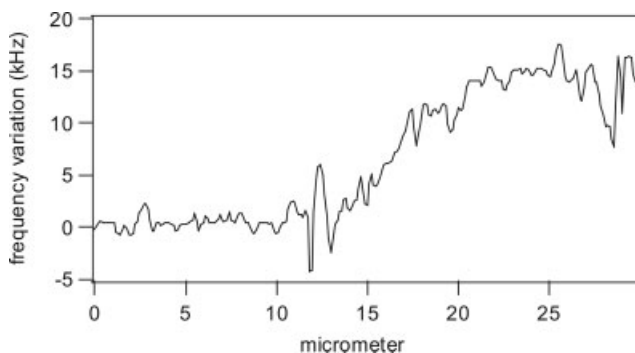


**Figure 7** Sample 2 frequency variation profile extracted from the frequency image of Figure 6. The frequency variation is displayed with a reference frequency equal to the mean frequency of the cantilever in the BR part (on the left).

transient decrease of the gain. The frequency and gain can then be changed without any modification of the mechanical properties of the material because of the scanning of the tip on a nonflat surface: the frequency and gain contrasts depend then on the roughness of the sample and the velocity of the tip; the frequency and gain are instead related to the derivative of the topography profile.

Second, for this reason, to obtain information independent of the topography, the mean resonance frequencies (mean gains) in the BR region on a flat area and in the SBR region on a flat area were compared. The comparison reveals unambiguously that the mechanical properties of the two elastomers are different. Moreover, it appears that the influence of the topography on the resonance frequency and gain variations is small compared with the influence of the nature of the elastomer: in the SBR part, the frequency variation is 2 kHz, and this value has to be compared to the frequency gap between BR and SBR (12 kHz).

Third, if the topography variations induce a gain change, it is possible to observe a gain or resonance frequency variation on a flat surface: close observation of the SBR part of each image shows, for example, that gain variations reveal more details than the topography images. Indeed, the gain variation is the

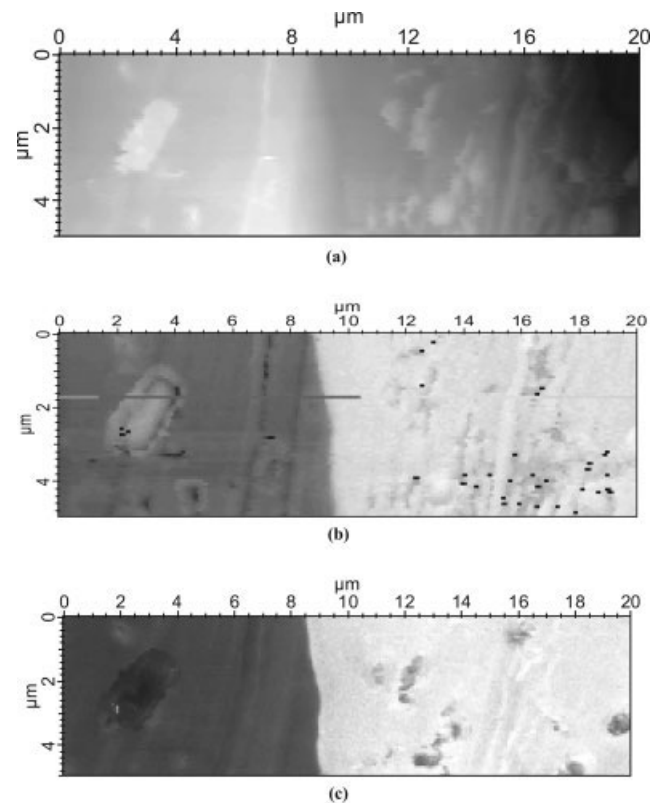


**Figure 8** (a) Topography, (b) frequency, and (c) gain images of sample 1 obtained with electrostatic excitation and with a sweeping frequency of 0.2 Hz.

result of a change for a fixed frequency of dissipated energy at the contact tip-sample.

In conclusion, even if the roughness and topography variation of the surface is strongly correlated to the gain and resonance frequency, the main source of the variation of the resonance frequency and the gain arises from the difference in the mechanical properties of the two elastomers. The roughness and topography induce only a second-order effect in comparison with the effect of the difference in the mechanical properties. It also should be noted that it is always possible to slow down the velocity of the tip on the surface, which decreases the topography-induced contrast of the gain and frequency images.

In the topography, phase, and gain images of sample 1 (Fig. 8), it also appears clear that the frequency image and gain image provide good evidence for the interface. The profile extracted from these image gives an interphase width equal to 100 nm according to the result obtained by phase measurements. It should be noted that in comparison with the tapping experiment, the solicitation of the elastomer in a contact-resonance experiment is very weak, and this confirms that the interphase width of 100 nm obtained by the phase measurement under hard tapping conditions is the true width.

### CONCLUSIONS

In this study, two methods have been presented to measure the interdiffusion at an interphase between two polymers in contact. The first is well-known tapping-mode AFM. Because of the frequently observed phase contrast inversion, it has been shown that both a high free amplitude (ca. 180 nm) and a reduced set point ratio are required to obtain good mechanical sensitivity and therefore a precise measurement of the interdiffusion. These particular conditions (hard mechanical solicitation) are allowed on very soft materials such as those studied. The interphase width has been precisely assessed between two miscible or immiscible polymers. These measurements have been confirmed by contact-resonance

microscopy (very weak mechanical solicitation), in which the tip in contact with the sample is electrostatically excited at the resonance frequency of the cantilever. The gain and frequency imaging have allowed us to precisely measure the interphase width between the same polymers. The same interphase widths are obtained by both methods (weak and hard mechanical solicitation), and this confirms that the true interphase width is measured.

### References

1. Cleveland, J. P.; Anczykowski, B.; Schmid, A. E.; Elings V. B. *Appl Phys Lett* 1998, 72, 2613.
2. Tamayo, J.; Garcia, R. *Appl Phys Lett* 1998, 73, 2926.
3. Achalla, P.; McCormick, J.; Hodge, T.; Moreland, C.; Esnault, P.; Karim, A.; Raghavan, D. *J Polym Sci Part B: Polym Phys* 2006, 44, 492.
4. Liu, R. Y. F.; Jin, Y.; Hiltner, A.; Baer, E. *Macromolecules* 2003, 24, 943.
5. Sanchez, M. S.; Mateo, J. M.; Colomer, F. J. R.; Gomez Ribelles, J. L. *Eur Polym J* 2006, 42, 1378.
6. Magonov, S. N.; Cleveland, J.; Elings, V.; Denley, D.; Wangboo, M. H. *Surf Sci* 1997, 389, 201.
7. Munz, M.; Cappella, B.; Sturm, H.; Geuss, M.; Schultz, E. *Adv Polym Sci* 2003, 164, 87.
8. Gao, S. L.; Mader, E. *Compos A* 2002, 33, 559.
9. Downing, T. D.; Kumar, R.; Cross, W. M.; Kjergtroen, L.; Kellar, J. J. *J Adhes Sci Technol* 2000, 14, 1801.
10. Round, A. N.; Miles, M. J. *Nanotechnology* 2004, 15, 5176.
11. Wang, Y.; Song, R.; Li, Y.; Shen, J. *Surf Sci* 2003, 530, 136.
12. Han, X.; Xu, J.; Liu, H. L.; Hu, Y. *Chin J Chem* 2006, 24, 149.
13. Raghavan, D.; VanLandingham, M.; Gu, X.; Nguyen, T. *Langmuir* 2000, 16, 9448.
14. Cuenot, S.; Duwez, A. S.; Martin, P.; Nysten, B. *Chim Nouvelle* 2002, 79, 89.
15. Wadu-Mesthrige, K.; Amro, N. A.; Garno, J. C.; Cruchon-Dupeyrat, S.; Liu, G. Y. *Appl Surf Sci* 2001, 175, 391.
16. Cuenot, S.; Fretigny, C.; Demoustier-Champagne, S.; Nysten, B. *J Appl Phys* 2003, 93, 5650.
17. Rabe, U.; Janser, K.; Arnold, W. *Rev Sci Instrum* 1996, 67, 3281.
18. Mazeran, P. E.; Loubet, J. Y. *Tribol Lett* 1997, 7, 199.
19. Durig, U.; Steinauer, H. R.; Blanc, N. *J Appl Phys Lett* 1997, 82, 3641.
20. Krok, F.; Kolodziej, J. J.; Such, B.; Czuba, P.; Struski, P.; Piatkowski, P.; Szymonski, M. *Surf Sci* 2004, 566, 63.
21. Garcia, R.; Perez R. *Surf Sci Rep* 2002, 47, 197.
22. Bodiguel, H.; Montes, H.; Fretigny, C. *Rev Sci Instrum* 2004, 75, 2529.